

Pyrrolic Type N Directed Borylation Route to BN-PAHs: Tuning the Photophysical Properties by Varying the Conjugation Shape and Size

Yanli Zhang, Chen Zhang, Yongkang Guo, Jincheng Ye, Bin Zhen, Yu Chen, and Xuguang Liu*

Cite This: *J. Org. Chem.* 2021, 86, 6322–6330

Read Online

ACCESS |

Metrics & More

Article Recommendations

Supporting Information

ABSTRACT: Two series of BN-cyclopenta[*a*]phenalenes have been synthesized through an indole/pyrrole oriented borylation reaction. A total of five compounds are obtained and fully characterized; one of them is unambiguously confirmed by single X-ray crystal structure. Their photophysical properties could be finely tuned through varying the conjugation size and shape of the bottom PAHs applied. Moreover, their response toward fluoride anions was also investigated.



INTRODUCTION

Polycyclic aromatic hydrocarbons (PAHs) are attractive candidates of functional materials in organic electronics, because of their unique properties.¹ Replacement of one or more C=C units in PAHs with the isoelectronic and isosteric B=N units resulted PAHs containing both boron and nitrogen atoms (BN-PAHs).² The idea is that introduction of BN units affects the steric attribute of the molecule slightly but will perturb the electronic structure and distribution within the molecule through introduction of a B=N dipole, offering a means tuning the properties of the materials relevant to function within optoelectronic devices.³ Recently, BN-PAHs have been verified for the huge potential applications in the field of organic light emitting diodes (OLEDs).^{3f–i}

The most popular methods for the synthesis of BN-PAHs are the intramolecular electrophilic C–H borylation of arenes and alkenes directed by nitrogen atoms.⁴ This is because the amine reacts with the boron source (boron halide reagent in most cases) to establish and anchor the B–N linkage, and the Lewis acidity of the boron center in this intermediate then facilitates the formation of the final BN heterocycle. The pioneering work on N-directed electrophilic borylation was first introduced by Dewar's group.⁵ There are three type of nitrogen atoms have been utilized as the directing group (Figure 1). C–H borylative cyclization of amino styrene or amino biphenyl type molecules, in which nitrogen in aniline is the directing group, resulted in a great number of BN-PAHs (Figure 1, top). There is a significant versatility in that a variety of R groups on the amine function can be accommodated, and the substitution on boron can also be manipulated. Recent efforts have resulted in significant progress for the synthesis of large size BN-PAHs.⁶ The second series is the pyridinic-type nitrogen-directed C–H borylation (Figure 1, middle), tetracoordinate boron was formed in most cases,⁷ few cases

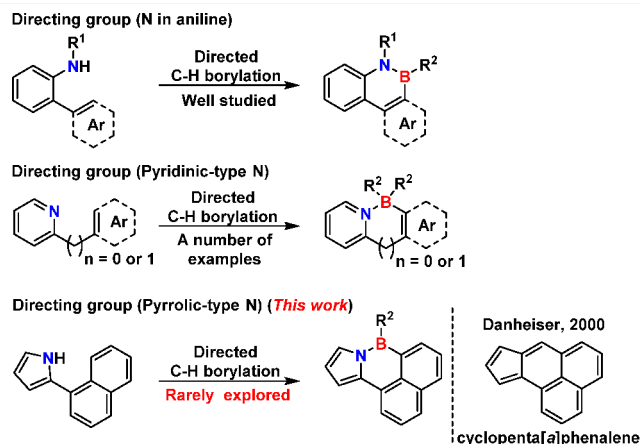


Figure 1. Three types of nitrogen atoms directed electrophilic C–H borylations.

demonstrated the tetracoordinate boron intermediate can be converted to tricoordinate boron.^{7e} The last series is the pyrrolic-type nitrogen directed C–H borylation, which has been rarely explored (Figure 1, bottom).^{3f,8} Pyrrolic-type N directed C–H borylation can lead to the formation of BN-cyclopenta[*a*]phenalene type molecule. Cyclopenta[*a*]phenalene is a class of nonalternant PAHs,⁹ which has been known back to the year of 2000.^{9a} We envisioned that

Received: January 19, 2021

Published: April 14, 2021



replacing C=C units with B=N units will cause this class of BN-heterocycles to have interesting photophysical properties. To the best of our knowledge, BN-cyclopenta[*a*]phenalene type molecules have not been reported to date. In addition, utilization of the pyrrolic-type N atom-oriented C–H borylation reaction can construct the BN-doped CP-PAHs rapidly with a pre-existed five-membered pyrrole ring in the starting material.

In this study, we describe the synthesis of a series of BN-cyclopenta[*a*]phenalene type molecules with linearly (naphthalene and anthracene) or nonlinearly (phenanthrene) fused rings, utilizing the pyrrolic-type N atoms-oriented C–H borylation reaction as the key step. Solid state structures and photophysical properties of the resulted PAHs are systematically investigated. The chemical structures of BN-cyclopenta[*a*]phenalenes are shown in Figure 1. Compounds **Py-Naph**, **Py-Phen** and **Py-Anth** contain a pyrrole unit, whereas indole subunit was included in the compounds **In-Naph**, **In-Phen** and **In-Anth** (Figure 2). Bottom part of these BN-cyclopenta[*a*]-

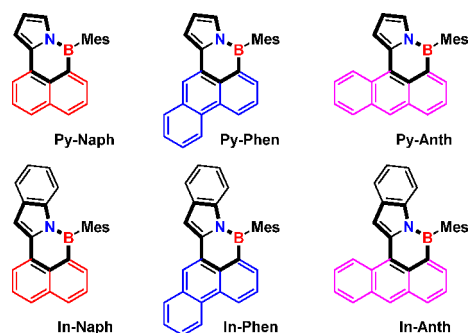


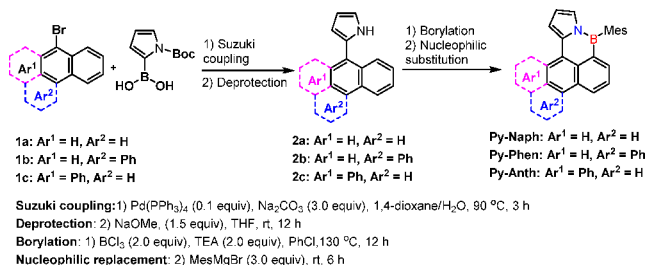
Figure 2. Chemical structures of pyrrole-based BN-PAHs **Py-Naph**, **Py-Phen**, and **Py-Anth** (top) and indole-based BN-PAHs **In-Naph**, **In-Phen**, and **In-Anth** (bottom).

phenalenes are the typical small PAHs, such as naphthalene (red), phenanthrene (blue) and anthracene (purple) respectively. The sterically hindered mesityl group was selected as the substitute on the boron to stabilize the final BN-PAHs.

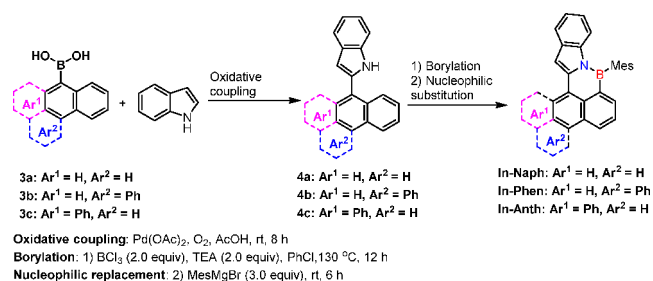
RESULTS AND DISCUSSION

We began our studies by synthesizing BN-cyclopenta[*a*]phenalenes using the coupling reaction, followed by the pyrrolic-type N atom-oriented C–H borylation reaction (Schemes 1 and 2). Cross coupling of brominated arenes with (1-(*tert*-butoxycarbonyl)-1*H*-pyrrol-2-yl)boronic acid, followed by deprotection of a Boc (*tert*-butoxycarbonyl) group generated the pyrrole substituted arene **2** in good yield (**2a**, 88.7%; **2b**, 72.1%; **2c**, 72.5%).¹⁰ The pyrrolic-type N

Scheme 1. Synthetic Route of Pyrrole-Based BN-PAHs **Py-Naph**, **Py-Phen**, and **Py-Anth**



Scheme 2. Synthetic Route of Indole-Based BN-PAHs **In-Naph**, **In-Phen**, and **In-Anth**



directed borylation occurred smoothly in the presence of Et₃N, furnishing the final BN-PAHs in moderate yields (**Py-Naph**, 71.9%; **Py-Phen**, 43.6%; **Py-Anth**, 16.8%).

We synthesized the indole-based BN-PAHs using a slightly different route. Precursors (**4**) were synthesized by the oxidative coupling the indole with brominated arenes (**4a**, 13.0%; **4b**, 28.1%; **4c**, 6.4%).¹¹ Unfortunately, the yield of this step is relatively low. Unidentified byproducts were observed in the reaction mixtures. To our delight, pyrrolic-type N atom-oriented C–H borylation went smoothly with moderate yields (**In-Naph**, 71.9%; **In-Phen**, 56.4%; **In-Anth**, 10.5%), using similar reaction conditions to the previous pyrrole-based PAHs. It should be noted the **In-Anth** is not very stable during purification, it decomposed slowly when exposed to air. Attempts using either the phenyl Grignard reagent or methyl Grignard reagent as the nucleophile failed to get the desired BN-PAHs, presumably due to the relatively smaller size of the phenyl or methyl ring, which is not bulky enough to stabilize the boron. We found that the fused bottom small PAHs play an important role in the stability of the final BN-PAHs. Naphthalene (**Py-Naph** and **In-Naph**) and phenanthrene (**Py-Phen** and **In-Phen**) fused derivatives with a mesityl group on boron are stable in air and could be purified by chromatography on silica gel. In contrast, anthracene fused derivatives (**Py-Anth** and **In-Anth**) are not stable in the air even with a large mesityl protecting group. Thermogravimetric analysis revealed that all five BN-cyclopenta[*a*]phenalenes have a decomposition temperature with 5% weight loss above 220 °C (See Figure S1, **Py-Naph**, 228 °C; **Py-Phen**, 279 °C; **Py-Anth**, 253 °C; **In-Naph**, 269 °C; **In-Phen**, 266 °C), indicating their good thermal stability.

All five compounds were fully characterized by ¹H NMR and ¹³C NMR, as well as the high-resolution mass spectrometry and FT-IR spectrometry. The formation of the six-membered BN heterocycles for **In-Naph** was further confirmed by X-ray crystallographic analysis. Single crystal of **In-Naph** was grown from a mixed solution of methanol, dichloromethane, and dimethylformamide; the data was analyzed by X-ray diffraction (Figure 3 and Table S1 in the Supporting Information).¹² The endocyclic B–N distance for **In-Naph** is 1.428(6) Å, which is sitting in between a BN dative interaction (approximate minimum: 1.601 Å) and BN double bond (approximate maximum: 1.408 Å),¹³ indicating a distinct double-bond character. The endocyclic B–C distance (1.551(7) Å) is comparable to that of an exocyclic B–C bond (1.567(6) Å). However, it is longer than B–C bonds in the most previously reported BN-PAHs by our group.¹⁴ The dihedral angle between the top phenyl ring (A ring) of indole and the bottom naphthalene ring (C ring) is 5.8°, which demonstrates the high planarity of the main scaffold. The mesityl is derived

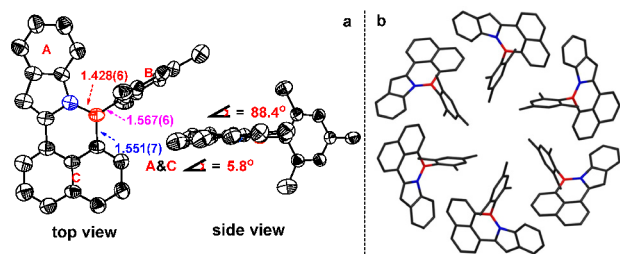


Figure 3. (a) Solid-state structures of BN-PAHs **In-Naph** with views parallel and perpendicular to the polycyclic planes (B red, N blue). Thermal ellipsoids are set at the 35% probability level for the structure on the left. Selected bond lengths (Å). H atoms have been omitted for clarity. (b) Crystal packing of **In-Naph** viewed along the *c*-axis.

from the mainframe with a dihedral angle of approximately 88.4° , which limits its conjugation with the mainframe. The mesityl group not only ensures that there are no aggregates in solid state because of their superior bulkiness but also provides an enhanced solubility. All compounds are soluble in the common solvents, such as toluene, dichloromethane, ethyl acetate, and tetrahydrofuran. The crystal packing diagram is shown in Figure 3b. A distinct propeller-shaped packing mode of **In-Naph** is observed through the *c*-axis. In total, six molecules comprise a circle, with mesityl groups toward the center of the circle.

In support the electron delocalization of the mainframe, nucleus independent chemical shift (NICS) calculations for the BN-PAHs were performed (Figures 4 and S2).¹⁵ The

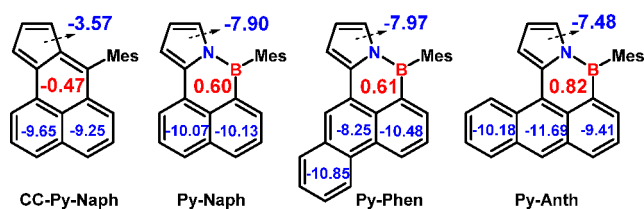


Figure 4. NICS(1) values (ppm) of **CC-Py-Naph**, **Py-Naph**, **Py-Phen**, and **Py-Anth** calculated at the GIAO-B3LYP/6-311G(d,p) level.

carbonaceous compound **CC-Py-Naph** was also involved for direct comparison. The NICS(1) values of the BN-containing rings in **Py-Naph**, **Py-Phen**, and **Py-Anth** show slightly positive values (**Py-Naph**, 0.60; **Py-Phen**, 0.61; **Py-Anth**, 0.82), indicating that all the BN-rings are nonaromatic. On the other hand, the NICS(1) value of the central ring in their carbonaceous counterpart shows slightly negative value (**CC-Py-Naph**, -0.47). Overall, the central ring of both the **CC-Py-Naph** and its BN-derivatives are nonaromatic, since all the NICS(1) values of the ring are close to zero. In addition, the NICS(1) values of the top pyrrole ring of **Py-Naph**, **Py-Phen**, and **Py-Anth** show a highly aromatic feature (**Py-Naph**, -7.90; **Py-Phen**, -7.97; **Py-Anth**, -7.48), whereas the NICS(1) value of the top five-member ring in **CC-Py-Naph** is -3.57, indicating weaker aromaticity as compared to its BN-analogue **Py-Naph**. It should be noted that the bottom ring in **Py-Naph** (-10.07, -10.13) displays more negative NICS(1) values than its all-carbon analogue **CC-Py-Naph** (-9.65, -9.25) as well. These results indicate that although **CC-Py-Naph** and its BN-embedded derivative **Py-Naph** possess the same π electrons in total, the (non)aromaticity of each ring is significantly

modified by the BN substitution. Moreover, the NICS(1) values of each rings of **In-Naph**, **In-Phen**, and **In-Anth** display similar trends (see Figure S2 in the Supporting Information).

To gain further insights into the electronic structures, we carried out the density functional theory (DFT) calculation of the six compounds, the frontier orbital shape and energy levels are shown in Figure 5. Taking the pyrrole series for example,

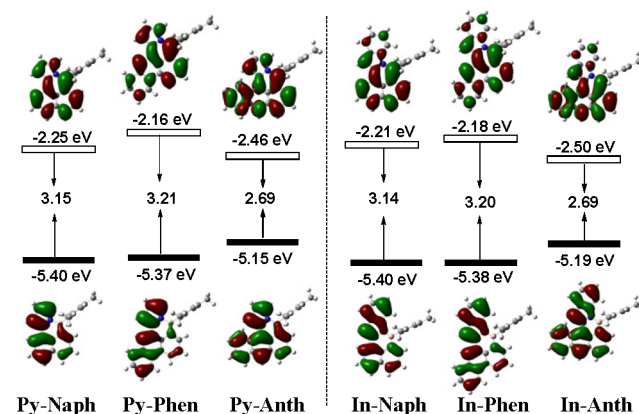


Figure 5. Frontier orbital maps and energy values (eV) of **Py-Naph**, **Py-Phen**, **Py-Anth**, **In-Naph**, **In-Phen**, and **In-Anth**. Determined at the B3LYP/6-311G(d,p) level of theory.

the HOMO and LUMO of all the three compounds are delocalized on the BN-PAHs main scaffold, no density on the mesityl substituents. The HOMO and LUMO levels are dependent on the different conjugation size and shape of the bottom PAHs, extended the bottom PAHs from naphthalene (**Py-Naph**) to the phenanthrene (**Py-Phen**) resulting in higher LUMO and HOMO energies. However, the anthracene derivative (**Py-Anth**) exhibits the lowest lying LUMO level (-2.46 eV) and highest lying HOMO level (-5.15 eV). Thus, **Py-Anth** shows the narrowest HOMO-LUMO gap (2.69 eV), which is in line with the red shift of its lower energy absorption band. The frontier orbital energy levels of more extended indole-derivatives are comparable with the pyrrole-derivatives. The calculated HOMO-LUMO gaps and frontier orbital energy levels of the indole series follow the same trends. In both series, naphthalene derivatives show the lowest lying LUMO level (**Py-Anth**, -2.46 eV; **In-Anth**, -2.50 eV) and highest lying HOMO level (**Py-Anth**, -5.15 eV; **In-Anth**, -5.19 eV). These results indicate that the electronic energies were greatly dependent on the nature of the fused PAHs on the bottom of the molecules. The higher HOMO level of **Py-Anth** and **In-Anth** might be the reason for diminishing their stability. We also carried out the DFT calculation on **CC-Py-Naph**, carbonaceous analog of **Py-Naph** (see Figure S3 in the Supporting Information). The replacement of the C=C unit with the isoelectronic and isosteric B=N unit resulted in a lower HOMO (**Py-Naph**, -5.40 eV; **CC-Py-Naph**, -5.26 eV) level and higher LUMO (**Py-Naph**, -2.25 eV; **CC-Py-Naph**, -2.64 eV) level, overall leading to a HOMO-LUMO gap opening of up to 0.53 eV. Similar phenomena were also reported in the literature of other BN-PAHs.^{14d,16}

Photophysical studies were carried out in cyclohexane (Figure 6 and Table 1). Compounds **Py-Phen** and **Py-Naph** exhibit similar absorption features. Furthermore, the comparison of the molar absorption coefficients of these two molecules shows that **Py-Naph** has roughly triple the

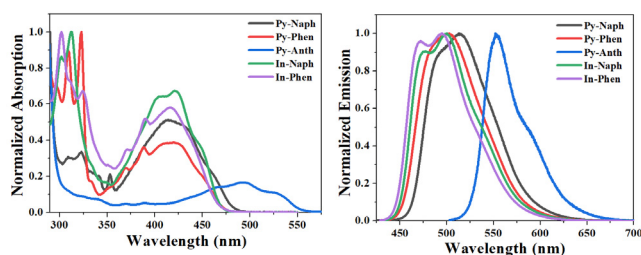


Figure 6. Normalized absorption (left) and emission (right) spectra of Py-Naph, Py-Phen, Py-Anth, In-Naph, and In-Phen in cyclohexane.

Table 1. Photophysical Properties of Py-Naph, Py-Phen, Py-Anth, In-Naph, and In-Phen in Cyclohexane

comp	λ_{abs}^a (nm)	ϵ ($M^{-1} \text{ cm}^{-1}$) (λ_{abs}^b)	λ_{em}^c (λ_{ex}^c) (nm)	$\Phi_{\text{pl}}^{d,e}$ (%)
Py-Naph	414, 353, 323	6400 (414)	515 (411)	0.76
Py-Phen	419, 323, 309	14600 (419)	501 (408)	0.54
Py-Anth	495	3800 (495)	553 (491)	0.10
In-Naph	421, 312	25200 (421)	499, 476 (420)	0.92
In-Phen	415, 324, 302	14300 (415)	494, 473 (419)	0.93

^aRefer to the intensity peak maxima values. ^bRefer to the lowest-energy peak maxima values. ^cRefer to the intensity peak maxima values. ^dAbsolute quantum yield in cyclohexane.

absorption intensity of **Py-Phen** at their major absorption band around 415 nm. In contrast, **Py-Anth** has a very different absorption feature. The absorption features of **Py-Anth** ($\lambda_{\text{abs}}^{\text{onset}} = 565$ nm) appear significantly bathochromically shifted of its longest wavelength in comparison with **Py-Naph** ($\lambda_{\text{abs}}^{\text{onset}} = 496$ nm) and **Py-Phen** ($\lambda_{\text{abs}}^{\text{onset}} = 483$ nm), which is consistent with the narrow HOMO–LUMO gap of **Py-Anth** predicted by the DFT calculation (Figure 5). As shown in Figure 5, the orbital contributions show that the phenyl ring of the indole moiety barely contributes to the LUMO in indole series, which is in line with the fact that indole series **In-Naph** and **In-Phen** exhibit a very similar absorption features as compared to their pyrrole counterparts **Py-Naph** and **Py-Phen**. It is a pity that the instability of the **In-Anth** inhibited its direct comparison with analogue **Py-Anth**.

All the five compounds emit in solution state (Figure 6, right). Emission maxima of pyrrole series decrease in the order **Py-Anth** > **Py-Naph** > **Py-Phen**. This trend is consistent with that observed in their absorption spectra. Different than the slightly structured emission of the pyrrole series, the indole series shows a structured emission spectrum. Interestingly, **In-Naph** and **In-Phen** experience a slight blue-shifted emission maxima, which is very abnormal considering they processes relatively larger conjugation sizes as compared to **Py-Naph** and **Py-Phen**. To gain further insights into the emission properties, we performed the calculations on the **Py-Naph** and its all-carbon analog **CC-Py-Naph** (Table S19–S21), since the experimental data of the carbonaceous analogs are not available in the literature. The calculated emission peak of **Py-Naph** was found at 495 nm, which attribute to the $S_1 \rightarrow S_0$ radiative transition ($f = 0.1248$). It is also consistent with the experimental values ($\lambda_{\text{em}} = 515$ nm). In contrast, the calculation showed that a strong band was found at 460 nm ($S_2 \rightarrow S_0$ transition, $f = 0.1926$) for **CC-Py-Naph**, along with a weak band at 637 nm ($S_1 \rightarrow S_0$ transition, $f = 0.0586$). Absolute fluorescence quantum yields were determined in

cyclohexane solution with integrating sphere. Except compound **Py-Anth** (0.10), quantum yields of all the other four compounds are very high, with the largest value determined for **In-Phen** (0.93), very closely followed by **In-Naph** (0.92), **Py-Naph** (0.76), and **Py-Phen** (0.54). Time-resolved measurements showed single-exponential decays for all five compounds, with lifetimes in the range of 9.1–20.2 ns (Figure S7 and Table S23). Moreover, the absorption and emission maxima are only slightly dependent on the polarity of the solvents (Figure S6). In addition, photophysical properties of these BN-PAHs in solid state were also investigated (Figure S11 and Table S24).

The electrochemical properties of **Py-Naph**, **Py-Phen**, **Py-Anth**, **In-Naph**, and **In-Anth** were investigated by cyclic voltammetry (Figure 7 and Figure S12). As displayed in Figure

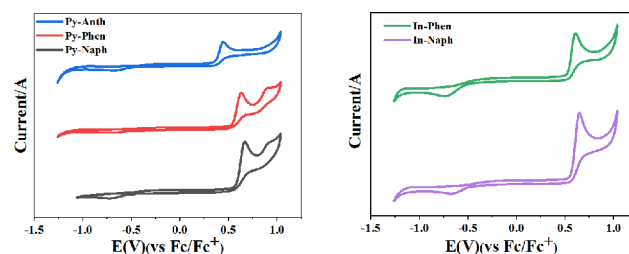


Figure 7. Cyclic voltammograms of **Py-Naph**, **Py-Phen**, **Py-Anth**, **In-Naph**, and **In-Anth** in dichloromethane (0.1 M *n*-Bu₄NPF₆ as supporting electrolyte; scan rate of 100 mV/s).

7, all five compounds exhibit irreversible oxidation processes without any well-developed reduction waves in dichloromethane. **Py-Naph** and **Py-Phen** present two oxidation processes at onset potentials of versus Fc/Fc⁺ (**Py-Naph**: 0.58, 0.86 V; **Py-Phen**: 0.53, 0.82 V). In contrast, **Py-Anth** presents only one obvious oxidation processes at onset potentials of versus Fc/Fc⁺ 0.37 V (Figure 7, left). The HOMO energy levels of **Py-Naph**, **Py-Phen**, and **Py-Anth** (−5.38, −5.32, −5.17 eV) could be evaluated by the equation $E_{\text{HOMO}} = -4.8 \text{ eV} - E_{\text{onset}}^{\text{ox}}$.¹⁷ Therefore, the LUMO levels can be deduced from the HOMO values and the optical band gaps (Table S23) are −2.88, −2.76, and −2.98 eV for **Py-Naph**, **Py-Phen**, and **Py-Anth**, respectively (Table S25). The trends of electrochemical properties deduced from the experiment are in good agreement with the calculation values (Table S26). It is unusual that **In-Naph** and **In-Phen** with enlarged π -skeletons present similar electrochemical behaviors with their pyrrole counterparts **Py-Naph** and **Py-Phen** (Figure 7 and Tables S25, S26).¹⁸

Tricoordinate organoboranes can accept a lone pair of electrons from a Lewis bases, resulting change their absorption and emission spectrum. Hence, some borane-based optical fluoride ions sensors were developed.¹⁹ We found that the addition of excess tetrabutylammonium fluoride (TBAF) to solutions of BN-PAHs **Py-Naph**, **Py-Phen**, **Py-Anth**, **In-Naph**, and **In-Anth** caused significant changes of their absorption and emission spectra (Figure 8 for **In-Naph** and Figure S8 for the other compounds). As shown in Figure 8, both the lower energy absorption band ($\lambda_{\text{abs}} = 418$ nm) and the higher energy band ($\lambda_{\text{abs}} = 312$ nm) of **In-Naph** were diminished upon addition of TBAF, generating a new higher energy band ($\lambda_{\text{abs}} = 380$ nm) at the same time (Figure 8, left). Like the change observed in the absorption spectra, the fluorescence intensity of the original band ($\lambda_{\text{em}} = 500$ nm) decreased dramatically,

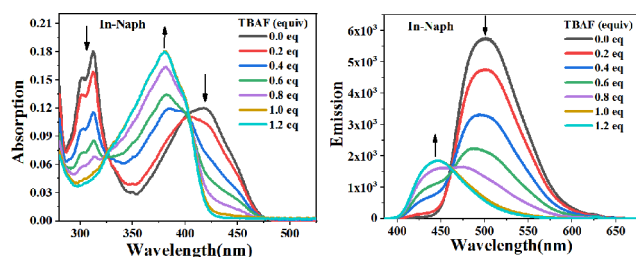


Figure 8. Absorption and emission spectra change upon adding TBAF to the solution of **In-Naph** ($c = 1 \times 10^{-5}$ M) in tetrahydrofuran. The excitation wavelength is 380 nm.

while a new emission band appeared at 444 nm. The binding constants of **In-Naph** toward fluoride ions in THF was determined as $\log K_a = 4.7 \pm 0.3$. The other four compounds showed similar response to TBAF as that of **In-Naph** (see Figure S8). We also monitored the fluoride addition of **Py-Phen** by ^{11}B NMR (Figure S9) and ^{19}F NMR (Figure S10). We found that the ^{11}B NMR signal change from 46.7 to 3.5 ppm, which indicates the formation of tetracoordinated boron. The ^{19}F NMR of the **Py-Phen** with TBAF (-139.7 ppm) was also different from the ^{19}F NMR signal of TBAF itself (-123.4 ppm).

CONCLUSIONS

In summary, five BN-cyclopenta[*a*]phenalene type molecules have been achieved via pyrrolic-type N atom-directed C–H borylation reaction. The (non)aromaticity of the BN-cyclopenta[*a*]phenalenes was quantified by computational and experimental investigations. In addition, the photophysical and electrochemical properties of these BN-cyclopenta[*a*]phenalenes were carefully studied, and their photophysical properties can be tuned by the fused small PAHs on the bottom of the scaffold. The method opens new possibilities to rapidly construct BN-doped cyclopenta-fused PAHs with rich photophysical properties. The preparation of other BN-PAHs using pyrrolic-type N atom-directed C–H borylation reaction is currently underway in our laboratory.

EXPERIMENTAL SECTION

General Methods. All oxygen- and moisture-sensitive manipulations were carried out under an inert atmosphere using either standard Schlenk techniques or a nitrogen-filled drybox. The heat source is an oil bath for reactions that requires heating.

THF, Et_2O , and toluene were purified by sodium absorption under argon. All other chemicals and solvents were purchased and used as received. 1-Naphthalene boronic acid, 9-phenanthrene boronic acid, 9-anthracene boronic acid, 1-bromonaphthalene, 9-bromophenanthrene, 9-bromoanthracene, triethylamine (extra dry, molecular sieve), 1-trimethylphenyl magnesium bromide (diethyl ether, 1.0 M), *N*-*boc*-2-pyrrolicboronic acid, and indole were purchased from Energy Chemical (Shanghai). Boron trichloride (toluene, 1.0 M) was purchased from Heowns (Tianjin, China). Petroleum ether, ethyl acetate, dichloromethane, ethanol, and THF were purchased from Hengshan Chemical (Tianjin, China). Toluene, Et_2O , acetic acid, and hydrochloric acid were purchased from Tianjin Chemical Reagent Company.

^1H NMR and ^{13}C NMR spectra were recorded on a Bruker AM-400. The reported chemical shifts were against TMS. The ^{11}B spectra were recorded on a Bruker AM-400 spectrometer, and the reported chemical shifts were against $\text{BF}_3 \cdot \text{Et}_2\text{O}$. High-resolution mass spectra were obtained with a micro mass GCT-TOF mass spectrometer. IR spectra were recorded on a Tensor 27 instrument with a Bruker OPTIK GmbH (Made in Germany) spectrometer.

The absorption spectra of all compounds were measured by Thermo Scientific Evolution 201 spectrophotometer. Fluorescence measurements were carried out with an F-7000 fluorescence spectrophotometer. Cyclic voltammetry (CV) was recorded on an electrochemical workstation of Shanghai (in China) ChenHua by CHI760E B17052. Data collections for compound **In-Naph** was performed at 113 K on a Rigaku Saturn CCD diffractometer using graphite-monochromated MoK radiation ($\lambda = 0.71073$ Å). Thermogravimetry (TG) was performed using a Netzsch TG-209 instrument. Samples were loaded into alumina crucible and heated at a constant rate of 10 °C/min under a nitrogen purge (20 mL/min).

Synthetic Procedures. *2-(Naphthalen-1-yl)-1H-pyrrole (2a)*. A flask containing $\text{Pd}(\text{PPh}_3)_4$ (278.5 mg, 0.24 mmol, 0.1 equiv), 1-(*tert*-butoxycarbonyl)-1H-pyrrol-2-yl)boronic acid (662.4 mg, 3.13 mmol, 1.3 equiv) and Na_2CO_3 (766.6 mg, 7.23 mmol, 3.0 equiv) was pumped and then refilled with nitrogen three times. 1-Bromonaphthalene (500.0 mg, 2.41 mmol, 1.0 equiv) and mixed solvent (1,4-dioxane/ $\text{H}_2\text{O} = 2/1$, 15 mL) was added to the above reaction mixture by syringe. The reaction mixture was heated to 100 °C and stirred for 4 h at the same temperature. The progress of the reaction was monitored by TLC. After the completion of the reaction was confirmed, the reaction mixture was cooled to room temperature and the solvent was removed. Then the reaction mixture was extracted with ethyl acetate three times and washed with water. The combined organic layers were then dried over Na_2SO_4 . After removal of solvents under reduced pressure, the MeONa (390.0 mg, 7.23 mmol, 3.0 equiv) was added and then refilled with nitrogen three times. The above mixture was dissolved in 10 mL anhydrous THF and stirred at room temperature for 5 h. Then the solvent was removed, and the reaction mixture was extracted with ethyl acetate and washed with water three times. The combined organic layers were then dried over Na_2SO_4 . After removal of solvents under reduced pressure, the mixture was purified by column chromatography on silica gel (using petroleum ether/ethyl acetate = 20/1 as eluent) to give the *2-(naphthalen-1-yl)-1H-pyrrole (2a)* as a light purple oil (416.0 mg, yield = 88.7%). The proton NMR is consistent with the reported data.²⁰

^1H NMR (400 MHz, CDCl_3): δ 8.36–8.38 (m, 2H, Ar), 7.94–7.96 (m, 1H, Ar), 7.85–7.87 (m, 1H, Ar), 7.51–7.58 (m, 4H, Ar), 6.95–6.98 (m, 1H, Ar), 6.59–6.61 (m, 1H, Ar), 6.48–6.49 (m, 1H, Ar).

*7-Mesityl-7H-naphtho[1,8-*cd*]pyrrolo[2,1-*f*][1,2]azaborinine (Py-Naph)*. Triethylamine (0.28 mL, 1.97 mmol, 2.0 equiv) and boron trichloride (1.0 M in toluene, 2.0 mL, 1.97 mmol, 2.0 equiv) were added in sequence into a sealed tube charged with a solution of *2-(naphthalen-1-yl)-1H-pyrrole (2a)*, 190.0 mg, 0.98 mmol, 1.0 equiv) in chlorobenzene (2 mL). The cap of the tube was quickly tightened, and the sealed tube was taken out of the glovebox. And, the reaction mixture was heated at 130 °C for 12 h. After cooling to room temperature, mesityl magnesium bromide (1.0 M in THF, 3 mL, 2.95 mmol, 3.0 equiv) was added under a nitrogen atmosphere to the reaction mixture and stirred at room temperature for another 8 h. Then, the mixture was quenched with water, and then solvent was removed by vacuum. The mixture was extracted with dichloromethane and washed with water. The combined organic layer was dried over MgSO_4 . After removal of the solvents, the residue was purified by column chromatography on silica gel (using petroleum ether/ethyl acetate = 20/1 as eluent) to give the **Py-Naph** as a yellow solid (226.2 mg, yield = 71.9%).

mp: 66–68 °C. ^1H NMR (400 MHz, CDCl_3): δ 8.17 (dd, $J_1 = 7.4$ Hz, 1H, Ar), 8.09 (dd, $J_1 = 8.2$ Hz, $J_2 = 1.0$ Hz, 1H, Ar), 7.88 (dd, $J_1 = 6.8$ Hz, $J_2 = 1.2$ Hz, 1H, Ar), 7.82 (d, $J = 8.0$ Hz, 1H, Ar), 7.62 (t, $J = 7.7$ Hz, 1H, Ar), 7.54 (dd, $J_1 = 8.1$ Hz, $J_2 = 6.8$ Hz, 1H, Ar), 7.14 (dd, $J_1 = 3.2$ Hz, $J_2 = 1.1$ Hz, 1H, Ar), 6.96 (s, 2H, Ar), 6.93 (dd, $J_1 = 2.9$ Hz, $J_2 = 1.0$ Hz, 1H, Ar), 6.52 (t, $J = 3.1$ Hz, 1H, Ar), 2.40 (s, 3H, CH_3), 2.13 (s, 6H, CH_3). $^{13}\text{C}\{^1\text{H}\}$ NMR (100 MHz, CDCl_3): δ 139.9, 139.8, 138.0, 134.9, 134.2, 132.5, 129.3, 128.0, 127.1, 126.9, 126.3, 126.2, 125.8, 122.3, 115.2, 109.5, 22.5, 21.3 (B-aryl carbons was not observed due to quadrupolar relaxation). ^{11}B NMR (128 MHz, $\text{BF}_3 \cdot \text{OEt}_2$): δ 46.7. FTIR (thin film): 702, 740, 772, 808, 844, 1030, 1068, 1120, 1268, 1312, 1338, 1368, 1414, 1446, 1504, 1556,

1578, 1610, 2856, 2920, 2964, 3046, 3096, 3414, 3476 cm^{-1} . HRMS (ESI-TOF) m/z calcd for $(\text{C}_{23}\text{H}_{21}\text{BN}) [\text{M} + \text{H}]^+$, 322.1762; found, 322.1766.

2-(Phenanthren-9-yl)-1H-pyrrole (2b). A flask containing Pd(PPh_3)₄ (224.2 mg, 0.19 mmol, 0.1 equiv), (1-(*tert*-butoxycarbonyl)-1H-pyrrol-2-yl)boronic acid (532.8 mg, 2.53 mmol, 1.3 equiv), 9-bromophenanthrene (502.2 mg, 1.94 mmol, 1.0 equiv), and Na_2CO_3 (618.7 mg, 5.83 mmol, 3.0 equiv) was pumped and then refilled with nitrogen three times. A mixed solvent (1,4-dioxane/ H_2O = 2/1, 15 mL) was added to the above mixture by syringe. The reaction mixture was heated to 100 °C and stirred for 4 h. The progress of the reaction was monitored by TLC. After the completion of the reaction was confirmed, the reaction mixture was cooled to room temperature and the solvent was removed. Then the reaction mixture was extracted with ethyl acetate and washed with water. The combined organic layers were then dried over Na_2SO_4 . After removal of solvents under reduced pressure, MeONa (315.0 mg, 5.83 mmol, 3.0 equiv) was added and then refilled with nitrogen three times. The above mixture was dissolved in 10 mL anhydrous THF and stirred at room temperature for 5 h. Then the solvent was removed and the reaction mixture was extracted with ethyl acetate and washed with water three times. The combined organic layers were then dried over Na_2SO_4 . After removal of solvents under reduced pressure, the mixture was purified by column chromatography on silica gel (using petroleum ether/ethyl acetate = 20/1 as eluent) to give the 2-(phenanthren-9-yl)-1H-pyrrole (2b) as a white solid (625.9 mg, yield = 72.1%). The proton NMR is consistent with the reported data.¹¹

¹H NMR (400 MHz, CDCl_3): δ 8.77 (d, J = 8.2 Hz, 1H, Ar), 8.70 (d, J = 8.2 Hz, 1H, Ar), 8.51 (br, 1H, NH), 8.35 (d, J = 8.2 Hz, 1H, Ar), 7.88 (dd, J_1 = 8.0 Hz, J_2 = 1.2 Hz, 1H, Ar), 7.78 (s, 1H, Ar), 7.54–7.74 (m, 4H, Ar), 7.01 (dd, J_1 = 4.1 Hz, J_2 = 2.6 Hz, 1H, Ar), 6.52–6.62 (m, 1H, Ar), 6.45 (dd, J_1 = 5.9 Hz, J_2 = 2.8 Hz, 1H, Ar).

8-Mesityl-8H-phenanthro[1,10-*cd*]pyrrolo[2,1-*f*][1,2]azaborinine (Py-Phen). Triethylamine (0.12 mL, 0.83 mmol, 2.0 equiv) and boron trichloride (1.0 M in toluene, 0.82 mL, 0.83 mmol, 2.0 equiv) were added in sequence into sealed tube charged with solution of 2-(phenanthren-9-yl)-1H-pyrrole (2b, 102.2 mg, 0.41 mmol, 1.0 equiv) in chlorobenzene (2 mL). The cap of tube was quickly tightened, and the sealed tube was taken out of the glovebox. And the reaction mixture was heated at 130 °C for 12 h. After cooling to room temperature, mesityl magnesium bromide (1.0 M in THF, 1.24 mL, 3.0 equiv) was added under nitrogen atmosphere and stirred for 12 h at room temperature. Then, the mixture was quenched with water, and then solvent was removed by vacuum. The mixture was extracted with dichloromethane and washed with water. The combined organic layer was dried over Na_2SO_4 and filtered. After removal of the solvents, the residue was purified by column chromatography on silica gel (using petroleum ether/ethyl acetate = 20/1 as eluent) to give the Py-Phen as yellow solid (66.4 mg, yield = 43.6%).

mp: 161–163 °C. ¹H NMR (400 MHz, CDCl_3): δ 8.98 (d, J = 7.7 Hz, 1H, Ar), 8.66–8.76 (m, 1H, Ar), 8.47 (s, 1H, Ar), 7.94–8.01 (m, 2H, Ar), 7.72 (dd, J_1 = 8.2 Hz, J_2 = 7.0 Hz, 1H, Ar), 7.63–7.67 (m, 2H, Ar), 7.28 (dd, J_1 = 3.2 Hz, J_2 = 1.1 Hz, 1H, Ar), 6.97 (s, 2H, Ar), 6.96 (dd, J_1 = 2.9 Hz, J_2 = 1.0 Hz, 1H, Ar), 6.57 (t, J = 3.1 Hz, 1H, Ar), 2.41 (s, 3H, CH_3), 2.14 (s, 6H, CH_3). ¹³C{¹H} NMR (100 MHz, CDCl_3): δ 139.9, 139.1, 138.1, 134.8, 132.1, 130.0, 129.7, 129.4, 128.7, 128.3, 127.2, 127.0, 126.6, 126.5, 126.1, 125.7, 123.0, 122.6, 115.5, 109.7, 22.5, 21.3 (B-aryl carbons was not observed due to quadrupolar relaxation). ¹¹B NMR (128 MHz, $\text{BF}_3 \cdot \text{OEt}_2$): δ 47.2. FTIR (thin film): 738, 806, 852, 1032, 1126, 1188, 1266, 1286, 1330, 1368, 1418, 1444, 1494, 1608, 2928 cm^{-1} . HRMS (ESI-TOF) m/z calcd for $(\text{C}_{27}\text{H}_{23}\text{BN}) [\text{M} + \text{H}]^+$, 372.1918; found, 372.1929.

2-(Anthracen-9-yl)-1H-pyrrole (2c). A flask containing Pd(PPh_3)₄ (224.2 mg, 0.19 mmol, 0.1 equiv), (1-(*tert*-butoxycarbonyl)-1H-pyrrol-2-yl)boronic acid (1c, 533.4 mg, 2.53 mmol, 1.3 equiv), 9-bromoanthracene (501.3 mg, 1.94 mmol, 1.0 equiv), and Na_2CO_3 (618.6 mg, 5.83 mmol, 3.0 equiv) was pumped and then refilled with nitrogen three times. A mixed solvent (1,4-dioxane/ H_2O = 2/1, 15 mL) was added to the above mixture by syringe. The reaction mixture was heated to 100 °C and stirred for 4 h. The progress of the reaction

was monitored by TLC. After the completion of the reaction was confirmed, the reaction mixture was cooled to room temperature and the solvent was removed. Then the reaction mixture was extracted with ethyl acetate and washed with water. The combined organic layers were then dried over Na_2SO_4 . After removal of solvents under reduced pressure, MeONa (315.0 mg, 5.83 mmol, 3.0 equiv) was added and then refilled with nitrogen three times. The above mixture was dissolved in 10 mL anhydrous THF and stirred at room temperature for 5 h. Then, the solvent was removed and the reaction mixture was extracted with ethyl acetate and washed with water three times. The combined organic layers were then dried over Na_2SO_4 . After removal of solvents under reduced pressure, the mixture was purified by column chromatography on silica gel (using petroleum ether/ethyl acetate = 20/1 as eluent) to give the 2-(anthracen-9-yl)-1H-pyrrole (2c) as a yellow solid (629.5 mg, yield = 72.5%). The proton NMR is consistent with the reported data.²¹

¹H NMR (400 MHz, CDCl_3): δ 8.47 (s, 1H, Ar), 8.25 (br, 1H, NH), 8.02 (d, J = 8.3 Hz, 2H, Ar), 7.94 (d, J = 8.8 Hz, 2H, Ar), 7.39–7.50 (m, 4H, Ar), 7.04 (dd, J_1 = 4.0, J_2 = 2.5 Hz, 1H, Ar), 6.55 (dd, J_1 = 5.9 Hz, J_2 = 2.8 Hz, 1H, Ar), 6.50–6.53 (m, 1H, Ar).

5-Mesityl-5H-anthra[1,9-*cd*]pyrrolo[2,1-*f*][1,2]azaborinine (Py-Anth). Triethylamine (0.12 mL, 0.83 mmol, 2.0 equiv) and boron trichloride (1.0 M in toluene, 0.84 mL, 0.83 mmol, 2.0 equiv) were added in sequence into a sealed tube charged with a solution of 2-(anthracen-9-yl)-1H-pyrrole (2c, 100.7 mg, 0.41 mmol, 1.0 equiv) in chlorobenzene (2 mL). The cap of the tube was quickly tightened, and the sealed tube was taken out of the glovebox. And the reaction mixture was heated at 130 °C for 12 h. After cooling to room temperature, mesityl magnesium bromide (1.0 M in THF, 1.24 mL, 3.0 equiv) was added under a nitrogen atmosphere and stirred for 12 h at room temperature. Then the mixture was quenched with water, and then solvent was removed by vacuum. The mixture was extracted with dichloromethane and washed with water. The combined organic layer was dried over Na_2SO_4 and filtered. After removal of the solvents, the residue was purified by column chromatography on silica gel (using petroleum ether/ethyl acetate = 20/1 as eluent) to give the Py-Anth as a red solid (25.0 mg, yield = 16.8%).

mp: 144–146 °C. ¹H NMR (400 MHz, CDCl_3): δ 9.10 (d, J = 9.0 Hz, 1H, Ar), 8.41 (s, 1H, Ar), 8.26 (d, J = 7.6 Hz, 1H, Ar), 8.10 (d, J = 8.4 Hz, 1H, Ar), 7.96 (dd, J_1 = 6.5 Hz, J_2 = 1.2 Hz, 1H, Ar), 7.62–7.67 (m, 1H, Ar), 7.51–7.58 (m, 3H, Ar), 7.07 (dd, J_1 = 3.0 Hz, J_2 = 0.9 Hz, 1H, Ar), 6.98 (s, 2H, Ar), 6.65 (t, J = 3.2 Hz, 1H, Ar), 2.42 (s, 3H, CH_3), 2.16 (s, 6H, CH_3). ¹³C{¹H} NMR (100 MHz, CDCl_3): δ 141.3, 140.1, 138.0, 135.1, 134.1, 132.6, 130.3, 129.5, 128.9, 127.6, 127.2, 127.1, 127.0, 126.5, 126.3, 125.33, 125.28, 124.1, 116.8, 115.2, 22.5, 21.3 (B-aryl carbons was not observed due to quadrupolar relaxation). ¹¹B NMR (128 MHz, $\text{BF}_3 \cdot \text{OEt}_2$): δ 45.6. FTIR (thin film): 738, 800, 844, 1028, 1092, 1122, 1168, 1292, 1334, 1368, 1414, 1456, 1524, 1556, 1610, 2856, 2918, 2962, 3049 cm^{-1} . HRMS (ESI-TOF) m/z calcd for $(\text{C}_{27}\text{H}_{23}\text{BN}) [\text{M} + \text{H}]^+$, 372.1918; found, 372.1922.

2-(Naphthalen-1-yl)-1H-indole (4a). Indole (1.0 g, 8.54 mmol, 1.0 equiv), 1-naphthylboronic acid (1.9 g, 11.1 mmol, 1.3 equiv), and Pd(OAc)₂ (191.6 mg, 0.9 mmol, 0.1 equiv) were added to a Schlenk flask. The mixture was pumped and then refilled with O_2 (1 atm) three times. AcOH (20 mL) was added by syringe, and the resulting solution stirred for 8 h at room temperature. Most of the AcOH was removed by distillation under reduced pressure, and a potassium carbonate aqueous solution was added slowly to neutralize the remaining acetic acid. The mixture was extracted with CH_2Cl_2 (150 mL), and washed with aqueous NaHCO_3 (2 × 60 mL). The organic layer was dried over Na_2SO_4 . After removal of the solvent, the residue was purified by flash chromatography on silica gel (using petroleum ether/ethyl acetate = 20/1 as eluent) to afford 2-(naphthalen-1-yl)-1H-indole (4a) as a white solid (350.8 mg, yield = 13.0%). The proton NMR is consistent with the reported data.²²

¹H NMR (400 MHz, CDCl_3): δ 8.31–8.36 (m, 2H, Ar), 7.88–7.96 (m, 2H, Ar), 7.73 (d, J = 7.4 Hz, 1H, Ar), 7.65 (dd, J_1 = 8.0 Hz, J_2 = 0.8 Hz, 1H, Ar), 7.50–7.58 (m, 3H, Ar), 7.46 (dd, J_1 = 8.0 Hz, J_2 = 0.8 Hz, 1H, Ar), 7.27 (td, J_1 = 7.08 Hz, J_2 = 1.2 Hz, 1H, Ar), 7.20 (td,

$J_1 = 7.6$ Hz, $J_2 = 1.1$ Hz, 1H, Ar), 6.82 (dd, $J_1 = 2.1$ Hz, $J_2 = 0.8$ Hz, 1H, Ar).

7-Mesityl-7H-naphtho[1',8':3,4,5][1,2]azaborinino[1,6-a]indole (In-Naph). Triethylamine (0.24 mL, 1.65 mmol, 2.0 equiv) and boron trichloride (1.0 M in toluene, 1.65 mL, 1.65 mmol, 2.0 equiv) were added in sequence into a sealed tube charged with a solution of 2-(naphthalen-1-yl)-1H-pyrrole (**4a**, 200.1 mg, 0.82 mmol, 1.0 equiv) in chlorobenzene (2 mL). The cap of the tube was quickly tightened, and the sealed tube was taken out from the glovebox. And, the reaction mixture was heated at 130 °C for 12 h. After cooling to room temperature, mesitylmagnesium bromide (1.0 M in THF, 2.47 mL, 3.0 equiv) was added under a nitrogen atmosphere and stirred for 8 h at room temperature. Then, the mixture was quenched with water, and then, solvent was removed by vacuum. The mixture was extracted with dichloromethane and washed with water. The combined organic layer was dried over Na_2SO_4 and filtered. After removal of the solvents, the residue was purified by column chromatography on silica gel (using petroleum ether/ethyl acetate = 20/1 as eluent) to give the **In-Naph** as a yellow solid (111.8 mg, yield = 71.9%).

mp: 210–212 °C. ^1H NMR (400 MHz, CDCl_3): δ 8.36 (d, $J = 7.4$ Hz, 1H, Ar), 8.06 (d, $J = 8.2$ Hz, 1H, Ar), 7.90 (d, $J = 8.0$ Hz, 1H, Ar), 7.78 (dd, $J_1 = 6.8$ Hz, $J_2 = 1.1$ Hz, 1H, Ar), 7.66 (t, $J = 7.7$ Hz, 2H, Ar), 7.50–7.54 (m, 1H, Ar), 7.51 (s, 1H, Ar), 7.21 (t, $J = 8.0$ Hz, 1H, Ar), 7.01 (s, 2H, Ar), 6.97–7.01 (m, 2H, Ar), 6.81 (d, $J = 7.9$ Hz, 1H, Ar), 2.46 (s, 3H, CH_3), 2.10 (s, 6H, CH_3). $^{13}\text{C}\{^1\text{H}\}$ NMR (101 MHz, CDCl_3): δ 141.3, 134.0, 139.2, 138.6, 138.1, 133.3, 132.48, 132.47, 130.5, 128.1, 127.9, 127.5, 126.6, 126.3, 123.7, 123.4, 123.3, 120.3, 114.9, 105.6, 22.1, 21.5 (B-aryl carbons was not observed due to quadrupolar relaxation). ^{11}B NMR (128 MHz, $\text{BF}_3 \cdot \text{OEt}_2$): δ 45.5. FTIR (thin film): 774, 806, 848, 900, 1032, 1090, 1138, 1166, 1216, 1262, 1336, 1378, 1450, 1500, 1610, 1636, 1658, 2924, 2853, 3367 cm^{-1} . HRMS (ESI-TOF) m/z calcd for ($\text{C}_{27}\text{H}_{23}\text{BN}$) $[\text{M} + \text{H}]^+$, 372.1918; found, 372.1913.

2-(Phenanthren-9-yl)-1H-indole (4b). Indole (1.0 g, 8.54 mmol, 1.0 equiv), 9-phenanthracenylboronic acid (2.5 g, 11.10 mmol, 1.3 equiv), and $\text{Pd}(\text{OAc})_2$ (191.6 mg, 0.85 mmol, 0.1 equiv) were added to a Schlenk flask. The mixture was pumped and then refilled with O_2 (1 atm) three times. AcOH (20 mL) was added by syringe, and the resulting solution was stirred for 8 h at room temperature. AcOH was removed by distillation under reduced pressure, and potassium carbonate aqueous solution was added slowly to neutralize the remaining acetic acid. The mixture was dissolved in CH_2Cl_2 (150 mL) and washed with aqueous NaHCO_3 (2 \times 60 mL). The organic layer was dried over Na_2SO_4 . After removal of the solvent, the product was purified by flash chromatography on silica gel eluting with ethyl acetate and petroleum ether (v:v = 1:20) to afford 2-phenanthren-9-yl-1H-indole (**4b**) as a white solid (350.8 mg, yield = 28.1%).

mp: 175–176 °C. ^1H NMR (400 MHz, CDCl_3): δ 8.79 (d, $J = 8.2$ Hz, 1H, Ar), 8.73 (d, $J = 8.2$ Hz, 1H, Ar), 8.39 (br, 1H, NH), 8.36 (dd, $J_1 = 8.2$ Hz, $J_2 = 0.8$ Hz, 1H, Ar), 7.90–7.93 (m, 2H, Ar), 7.68–7.76 (m, 3H, Ar), 7.59–7.66 (m, 2H, Ar), 7.47 (dd, $J_1 = 8.0$ Hz, $J_2 = 0.6$ Hz, 1H), 7.28 (td, $J_1 = 7.1$ Hz, $J_2 = 1.1$ Hz, 1H, Ar), 7.21 (td, $J_1 = 8.7$ Hz, $J_2 = 1.0$ Hz, 1H, Ar), 6.86 (d, $J = 1.2$ Hz, 1H). $^{13}\text{C}\{^1\text{H}\}$ NMR (100 MHz, CDCl_3): δ 136.7, 136.3, 131.3, 130.7, 130.6, 130.2, 129.8, 128.82, 128.80, 128.3, 127.2, 127.03, 126.97, 126.86, 126.5, 123.0, 122.6, 122.3, 120.6, 120.2, 110.9, 103.9. FTIR (thin film): 3410, 3054, 1452, 1306, 1046, 1018, 798, 744 cm^{-1} . HRMS (ESI-TOF) m/z calcd for ($\text{C}_{22}\text{H}_{16}\text{N}$) $[\text{M} - \text{H}]^-$, 292.1132; found 292.1128.

8-Mesityl-8H-phenanthro[1',10':3,4,5][1,2]azaborinino[1,6-a]indole (In-Phen). Triethylamine (0.1 mL, 0.7 mmol, 2.0 equiv) and boron trichloride (1.0 M in toluene, 0.7 mL, 0.7 mmol, 2.0 equiv) were added in sequence into a sealed tube charged with solution of 2-(phenanthren-9-yl)-1H-indole (**4b**, 109.0 mg, 0.3 mmol, 1.0 equiv) in toluene (3 mL). The cap of the tube was quickly tightened, and the sealed tube was taken out of the glovebox. And the reaction mixture was heated at 110 °C for 12 h. After cooling to room temperature, mesitylmagnesium bromide (1.0 M in THF, 1.0 mL, 2.0 equiv) was added under a nitrogen atmosphere and stirred for 12 h at room temperature. Then the mixture was quenched with water, and then, the solvent was removed by vacuum. The mixture was extracted with

dichloromethane and washed with water. The combined organic layer was dried over MgSO_4 and filtered. After removal of the solvents, the residue was purified by column chromatography on silica gel (using petroleum ether/ethyl acetate = 20/1 as eluent) to give the compound **In-Phen** as a yellow solid (80.8 mg, yield = 56.4%).

mp: 156–158 °C. ^1H NMR (400 MHz, CDCl_3): δ 8.94 (d, $J = 8.3$ Hz, 1H, Ar), 8.72 (d, $J = 7.4$ Hz, 1H, Ar), 8.68 (s, 1H, Ar), 7.98–8.07 (m, 1H, Ar), 7.88 (dd, $J_1 = 6.8$ Hz, $J_2 = 1.0$ Hz, 1H, Ar), 7.64–7.75 (m, 5H, Ar), 7.20–7.25 (m, 1H, Ar), 7.03 (s, 2H, Ar), 6.98–7.02 (m, 1H, Ar), 6.81 (d, $J = 8.3$ Hz, 1H, Ar), 2.47 (s, 3H, CH_3), 2.11 (s, 6H, CH_3). $^{13}\text{C}\{^1\text{H}\}$ NMR (100 MHz, CDCl_3): δ 141.2, 139.9, 139.2, 138.1, 132.5, 131.9, 130.4, 130.2, 129.3, 129.0, 127.7, 127.6, 127.11, 127.06, 127.0, 126.1, 124.5, 123.7, 123.3, 122.7, 120.3, 114.9, 105.7, 22.2, 21.5 (B-aryl carbons was not observed due to quadrupolar relaxation). ^{11}B NMR (128 MHz, $\text{BF}_3 \cdot \text{OEt}_2$): δ 45.9. FTIR (thin film): 846, 1030, 1070, 1102, 1140, 1166, 1192, 1262, 1282, 1340, 1374, 1452, 1490, 1554, 1608, 2856, 2918, 3049, 3414, 3474 cm^{-1} . HRMS (ESI-TOF) m/z calcd for ($\text{C}_{31}\text{H}_{23}\text{BN}$) $[\text{M} + \text{H}]^+$, 422.2075; found, 422.2078.

2-(Anthracen-9-yl)-1H-indole (4c). Indole (1.0 g, 8.5 mmol, 1.5 equiv), 9-anthracenylboronic acid (1.3 g, 5.7 mmol, 1.0 equiv), and $\text{Pd}(\text{OAc})_2$ (256.0 mg, 1.1 mmol, 0.2 equiv) were added to a Schlenk flask. The mixture was pumped and then refilled with O_2 (1 atm) three times. AcOH (20 mL) was added by syringe and resulting solution was stirred for 8 h at room temperature. AcOH was removed by distillation under reduced pressure, and potassium carbonate aqueous solution was added slowly to neutralize remaining acetic acid. And, the residue was dissolved in CH_2Cl_2 (150 mL) and washed with aqueous NaHCO_3 (2 \times 60 mL). The organic layer was dried over Na_2SO_4 . After removal of the solvent, the crude product was purified by flash chromatography on silica gel eluting with ethyl acetate and petroleum ether (v:v = 1:20) to afford 2-(anthracen-9-yl)-1H-indole (**4c**) as a white solid (160.0 mg, yield = 6.4%). The proton NMR is consistent with the reported data.¹¹

^1H NMR (400 MHz, CDCl_3): δ 8.54 (s, 1H, Ar), 8.46 (br, 1H, NH), 8.09 (d, $J = 8.5$ Hz, 2H, Ar), 7.92 (d, $J = 8.8$ Hz, 2H, Ar), 7.56 (d, $J = 8.2$ Hz, 1H, Ar), 7.48 (t, $J = 7.36$ Hz, 2H, Ar), 7.37 (d, $J = 2.3$ Hz, 1H, Ar), 7.28–7.36 (m, 3H, Ar), 7.15 (d, $J = 7.8$ Hz, 1H, Ar), 7.08 (t, $J = 11.0$ Hz, 1H, Ar).

9-Mesityl-9H-anthra[1',9':3,4,5][1,2]azaborinino[1,6-a]indole (In-Anth). Triethylamine (0.1 mL, 0.68 mmol, 2.0 equiv) and boron trichloride (1.0 M in toluene, 0.68 mL, 0.68 mmol, 2.0 equiv) were added in sequence into sealed tube charged with solution of 2-(9-anthracenyl)-1H-indole (**4c**, 100.2 mg, 0.34 mmol, 1.0 equiv) in toluene (3 mL). The cap of the tube was quickly tightened, and the sealed tube was taken out from the glovebox. And, the reaction mixture was heated at 110 °C for 12 h. After cooling to room temperature, mesitylmagnesium bromide (1.0 M in THF, 1.0 mL, 3.0 equiv) was added under a nitrogen atmosphere and stirred for 12 h at room temperature. Then, the mixture was quenched with water, and then, the solvent was removed by vacuum. The mixture was extracted with dichloromethane and washed with water. The combined organic layer was dried over MgSO_4 and filtered. After removal of the solvents, the residue was purified by column chromatography on silica gel (using petroleum ether/ethyl acetate = 20/1 as eluent) to give the **In-Anth** as a red solid (15.8 mg, yield = 10.5%). It decomposed gradually toward air. The ^{13}C NMR was not recorded due to its instability. Please note that we ran the reaction several times and pure product was not guaranteed each time by the method mentioned above, presumably due to its instability.

^1H NMR (400 MHz, CDCl_3): δ 8.94 (d, $J = 7.6$ Hz, 1H, Ar), 8.72 (d, $J = 7.3$ Hz, 1H, Ar), 8.68 (s, 1H, Ar), 8.02–8.06 (m, 1H, Ar), 7.88 (d, $J = 6.9$ Hz, 1H, Ar), 7.65–7.74 (m, 5H, Ar), 7.23 (t, $J = 7.5$ Hz, 1H, Ar), 7.03 (s, 2H, Ar), 6.98–7.02 (m, 1H, Ar), 6.82 (d, $J = 8.2$ Hz, 1H, Ar), 2.47 (s, 3H, CH_3), 2.11 (s, 6H, CH_3).

■ ASSOCIATED CONTENT

■ Supporting Information

The Supporting Information is available free of charge at <https://pubs.acs.org/doi/10.1021/acs.joc.1c00142>.

NMR spectra, UV–vis and photoluminescence data, X-ray crystallographic data, and theoretical calculations. Experimental and computational details (PDF)

■ Accession Codes

CCDC 2053243 contains the supplementary crystallographic data for this paper. These data can be obtained free of charge via www.ccdc.cam.ac.uk/data_request/cif, or by emailing data_request@ccdc.cam.ac.uk, or by contacting The Cambridge Crystallographic Data Centre, 12 Union Road, Cambridge CB2 1EZ, UK; fax: +44 1223 336033.

■ AUTHOR INFORMATION

■ Corresponding Author

Xuguang Liu – Tianjin Key Laboratory of Organic Solar Cells and Photochemical Conversion, Tianjin Key Laboratory of Drug Targeting and Bioimaging, School of Chemistry and Chemical Engineering, Tianjin University of Technology, Tianjin 300384, People's Republic of China; Key Laboratory of Synthetic and Self-Assembly Chemistry for Organic Functional Molecules, Shanghai Institute of Organic Chemistry, Chinese Academy of Sciences, Shanghai 200032, People's Republic of China; orcid.org/0000-0002-7859-3139; Email: xuguangliu@tjut.edu.cn

■ Authors

Yanli Zhang – Tianjin Key Laboratory of Organic Solar Cells and Photochemical Conversion, Tianjin Key Laboratory of Drug Targeting and Bioimaging, School of Chemistry and Chemical Engineering, Tianjin University of Technology, Tianjin 300384, People's Republic of China

Chen Zhang – Tianjin Key Laboratory of Organic Solar Cells and Photochemical Conversion, Tianjin Key Laboratory of Drug Targeting and Bioimaging, School of Chemistry and Chemical Engineering, Tianjin University of Technology, Tianjin 300384, People's Republic of China

Yongkang Guo – Tianjin Key Laboratory of Organic Solar Cells and Photochemical Conversion, Tianjin Key Laboratory of Drug Targeting and Bioimaging, School of Chemistry and Chemical Engineering, Tianjin University of Technology, Tianjin 300384, People's Republic of China

Jincheng Ye – Tianjin Key Laboratory of Organic Solar Cells and Photochemical Conversion, Tianjin Key Laboratory of Drug Targeting and Bioimaging, School of Chemistry and Chemical Engineering, Tianjin University of Technology, Tianjin 300384, People's Republic of China

Bin Zhen – Tianjin Key Laboratory of Organic Solar Cells and Photochemical Conversion, Tianjin Key Laboratory of Drug Targeting and Bioimaging, School of Chemistry and Chemical Engineering, Tianjin University of Technology, Tianjin 300384, People's Republic of China

Yu Chen – Tianjin Key Laboratory of Organic Solar Cells and Photochemical Conversion, Tianjin Key Laboratory of Drug Targeting and Bioimaging, School of Chemistry and Chemical Engineering, Tianjin University of Technology, Tianjin 300384, People's Republic of China; orcid.org/0000-0003-1314-5316

Complete contact information is available at: <https://pubs.acs.org/doi/10.1021/acs.joc.1c00142>

■ Notes

The authors declare no competing financial interest.

■ ACKNOWLEDGMENTS

We gratefully acknowledge the financial support from the National Natural Science Foundation of China (22071181, 21502140), Natural Science Foundation of Tianjin (17JCZDJC37700, 18JCQNJC06900), Tianjin University of Technology, and the Shanghai Institute of Organic Chemistry (K2015-10). We thank the Training Project of Innovation Team of Colleges and Universities in Tianjin (TD13-5020). We also thank Prof. Xiaoming Wu and Mr. Mingkuan Cui at Tianjin University of Technology for assistance on studies of photophysical properties in solid state.

■ REFERENCES

- (1) (a) Zeng, Z. B.; Shi, X. L.; Chi, C. Y.; López Navarrete, J. T.; Casado, J.; Wu, J. S. Pro-aromatic and anti-aromatic π -conjugated molecules: an irresistible wish to be diradicals. *Chem. Soc. Rev.* **2015**, *44*, 6578–6596. (b) Anthony, J. E. Functionalized acenes and heteroacenes for organic electronics. *Chem. Rev.* **2006**, *106*, 5028–5048. (c) Hirai, M.; Tanaka, N.; Sakai, M.; Yamaguchi, S. Structurally constrained boron-, nitrogen-, silicon-, and phosphorus-centered polycyclic π -conjugated systems. *Chem. Rev.* **2019**, *119*, 8291–8331. (d) Pascal, R. A., Jr. Twisted Acenes. *Chem. Rev.* **2006**, *106*, 4809–4819. (e) Ishibashi, J. S. A.; Darrigan, C.; Chrostowska, A.; Li, B.; Liu, S.-Y. A BN anthracene mimics the electronic structure of more highly conjugated systems. *Dalton Trans.* **2019**, *48*, 2807–2812.
- (2) (a) Pei, J.; Zhuang, F. D.; Wang, J. Y. Recent progress and challenges in the synthesis of boron-nitrogen fused polycyclic aromatic hydrocarbons. *Zhongguo Kexue: Huaxue* **2020**, *50*, 1205–1216. (b) Campbell, P. G.; Marwitz, A. J. V.; Liu, S.-Y. Recent advances in azaborine chemistry. *Angew. Chem., Int. Ed.* **2012**, *51*, 6074–6092. (c) Giustra, Z. X.; Liu, S.-Y. The state of the art in azaborine chemistry: new synthetic methods and applications. *J. Am. Chem. Soc.* **2018**, *140*, 1184–1194. (d) Morgan, M. M.; Piers, W. E. Efficient synthetic methods for the installation of boron-nitrogen bonds in conjugated organic molecules. *Dalton. Trans.* **2016**, *45*, 5920–5924. (e) Appiaris, Y.; Stauch, T.; Lork, E.; Rusch, P.; Bigall, N. C.; Staubitz, A. From a 1,2-azaborinine to large BN-PAHs via electrophilic cyclization: synthesis, characterization and promising optical properties. *Org. Chem. Front.* **2021**, *8*, 10–17.
- (3) Reviews, see: (a) Wang, J. Y.; Pei, J. BN-embedded aromatics for optoelectronic applications. *Chin. Chem. Lett.* **2016**, *27*, 1139–1146. (b) Wang, X. Y.; Wang, J. Y.; Pei, J. BN heterosuperbenzenes: synthesis and properties. *Chem. - Eur. J.* **2015**, *21*, 3528–3539. (c) Huang, J.; Li, Y. BN embedded polycyclic π -conjugated systems: synthesis, optoelectronic properties, and photovoltaic applications. *Front. Chem.* **2018**, *6*, 341 Selected recent examples, see: (d) Huang, H.; Zhou, Y.; Wang, Y.; Cao, X.; Han, C.; Liu, G.; Xu, Z.; Zhan, C.; Hu, H.; Peng, Y.; Yan, P.; Cao, D. Precise molecular design for BN-modified polycyclic aromatic hydrocarbons toward mechanochromic materials. *J. Mater. Chem. A* **2020**, *8*, 22023–22031. (e) Wang, X.; Sun, Z.; Ding, K.; Qiang, P.; Zhu, W.; Han, S.; Zhang, F. Concise approach to T-shaped NBN-phenalene cored luminogens as intensive blue light emitters. *Chem. - Eur. J.* **2020**, *26*, 13966–13972. (f) Yang, D.-T.; Nakamura, T.; He, Z.; Wang, X.; Wakamiya, A.; Peng, T.; Wang, S. Doping polycyclic arenes with nitrogen-boron-nitrogen (NBN) units. *Org. Lett.* **2018**, *20*, 6741–6745. (g) Qiang, P.; Sun, Z.; Wan, M.; Wang, X.; Thiruvengadam, P.; Bingi, C.; Wei, W.; Zhu, W.; Wu, D.; Zhang, F. Successive annulation to fully zigzag-edged polycyclic heteroaromatic hydrocarbons with strong blue-green electroluminescence. *Org. Lett.* **2019**, *21*, 4575–4579. (h) Fu, Y.; Zhang, K.; Dmitrieva, E.; Liu, F.; Ma, J.; Weigand, J. J.; Popov, A. A.; Berger, R.; Pisula, W.; Liu, J.; Feng, X. NBN-embedded polycyclic aromatic hydrocarbons containing pentagonal and heptagonal rings. *Org. Lett.* **2019**, *21*, 1354–1358. (i) Sun, Z.; Yi, C.; Liang, Q.; Bingi,

C.; Zhu, W.; Qiang, P.; Wu, D.; Zhang, F. π -Extended C_2 -symmetric double NBN-heterohelicenes with exceptional luminescent properties. *Org. Lett.* **2020**, *22*, 209–213.

(4) Iqbal, S. A.; Pahl, J.; Yuan, K.; Ingleson, M. J. Intramolecular (directed) electrophilic C-H borylation. *Chem. Soc. Rev.* **2020**, *49*, 4564–4591.

(5) Dewar, M. J. S.; Kubba, V. P.; Pettit, R. New heteroaromatic compounds. part I. 9-Axa-10-boraphenanthrene. *J. Chem. Soc.* **1958**, 3073–3076.

(6) (a) Sun, C. J.; Wang, N.; Peng, T.; Yin, X.; Wang, S.; Chen, P. BN-functionalized benzotrithiophene-based azaborines: synthesis, structures, and anion binding properties. *Inorg. Chem.* **2019**, *58*, 3591–3595. (b) Zhuang, F. D.; Sun, Z. H.; Yao, Z. F.; Chen, Q. R.; Huang, Z.; Yang, J. H.; Wang, J. Y.; Pei, J. BN-embedded tetrabenzopentacene: a pentacene derivative with improved stability. *Angew. Chem., Int. Ed.* **2019**, *58*, 10708–10712. (c) Chen, Y.; Chen, W.; Qiao, Y.; Lu, X.; Zhou, G. BN-embedded polycyclic aromatic hydrocarbon oligomers: synthesis, aromaticity, and reactivity. *Angew. Chem., Int. Ed.* **2020**, *59*, 7122–7130. (d) Pati, P. B.; Jin, E.; Kim, Y.; Kim, Y.; Mun, J.; Kim, S. J.; Kang, S. J.; Choe, W.; Lee, G.; Shin, H. J.; Park, Y. S. Unveiling 79-year-old ixene and its BN-doped derivative. *Angew. Chem., Int. Ed.* **2020**, *59*, 14891–14895. (e) Hatakeyama, T.; Hashimoto, S.; Oba, T.; Nakamura, M. Azaboradibenzo[6]helicene: carrier inversion induced by helical homochirality. *J. Am. Chem. Soc.* **2012**, *134*, 19600–19603. (f) Haque, A.; Al-Balushi, R. A.; Raithby, P. R.; Khan, M. S. Recent Advances in π -Conjugated \dot{N} C-Chelate Organoboron Materials. *Molecules* **2020**, *25*, 2645–2666.

(7) (a) Ishida, N.; Moriya, T.; Goya, T.; Murakami, M. Synthesis of pyridine-borane complexes via electrophilic aromatic borylation. *J. Org. Chem.* **2010**, *75*, 8709–8712. (b) Zhang, Z.; Wang, Y.; Wang, W.; Yamamoto, Y.; Bao, M.; Yu, X. Convenient synthesis of tetracoordinated organoboron compounds via C-H borylation of aryl-N-heteroaromatics with TfOBnBu₂. *Tetrahedron Lett.* **2020**, *61*, 152199. (c) Vanga, M.; Lalancette, R. A.; Jäkle, F. Controlling the optoelectronic properties of pyrene by regioselective lewis base-directed electrophilic aromatic borylation. *Chem. - Eur. J.* **2019**, *25*, 10133–10140. (d) Yoshigoe, Y.; Kuninobu, Y. Iron-catalyzed ortho-selective C-H borylation of 2-phenylpyridines and their analogs. *Org. Lett.* **2017**, *19*, 3450–3453. (e) Kunchala, D.; Sa, S.; Nayak, P.; Ponniah S, J.; Venkatasubbaiah, K. Tetrahydrodibenzophenanthridine-based boron-bridged polycyclic aromatic hydrocarbons: synthesis, structural diversity, and optical properties. *Organometallics* **2019**, *38*, 870–878. (f) Liu, K.; Lalancette, R. A.; Jakle, F. Tuning the structure and electronic properties of B-N fused dipyrindylanthracene and implications on the self-sensitized reactivity with singlet oxygen. *J. Am. Chem. Soc.* **2019**, *141*, 7453–7462. (g) Lu, H.; Nakamura, T.; Yamashita, K.; Yanagisawa, H.; Nureki, O.; Kikkawa, M.; Gao, H.; Tian, J.; Shang, R.; Nakamura, E. B/N-doped p-arylenevinylene chromophores: synthesis, properties, and microcrystal electron crystallographic study. *J. Am. Chem. Soc.* **2020**, *142*, 18990–18996. (h) Crossley, D. L.; Cid, J.; Curless, L. D.; Turner, M. L.; Ingleson, M. J. Facile arylation of four-coordinate boron halides by borenium cation mediated boro-desilylation and -destannylation. *Organometallics* **2015**, *34*, 5767–5774. (i) Zhu, C.; Guo, Z.-H.; Mu, A. U.; Liu, Y.; Wheeler, S. E.; Fang, L. Low band gap coplanar conjugated molecules featuring dynamic intramolecular Lewis acid–base coordination. *J. Org. Chem.* **2016**, *81*, 4347–4352.

(8) Wang, X. Y.; Yang, D. C.; Zhuang, F. D.; Liu, J. J.; Wang, J. Y.; Pei, J. Postfunctionalization of BN-embedded polycyclic aromatic compounds for fine-tuning of their molecular properties. *Chem. - Eur. J.* **2015**, *21*, 8867–8873.

(9) (a) Shea, K. M.; Lee, K. L.; Danheiser, R. L. Synthesis and properties of 9-Alkyl- and 9-arylcyclopenta[a]phenalenes. *Org. Lett.* **2000**, *2*, 2353–2356. (b) Du, Y.; Wang, L.; Plunkett, K. N. 1,1'-Biaceanthrylene and 2,2'-biaceanthrylene: models for linking larger polycyclic aromatic hydrocarbons via five-membered rings. *J. Org. Chem.* **2020**, *85*, 79–84. (c) Chase, D. T.; Fix, A. G.; Kang, S. J.; Rose, B. D.; Weber, C. D.; Zhong, Y.; Zakharov, L. N.; Lonergan, M. C.; Nuckolls, C.; Haley, M. M. 6,12-Diarylindeno[1,2-b]fluorenes:

syntheses, photophysics, and ambipolar OFETs. *J. Am. Chem. Soc.* **2012**, *134*, 10349–10352.

(10) (a) Nakazono, M.; Saita, K.; Oshikawa, Y.; Tani, K.; Nanbu, S.; Zaitso, K. Fluorescence properties of 2-aryl substituted indoles. *Spectrochim. Acta, Part A* **2011**, *78*, 905–908. (b) Ravinder, K.; Reddy, A. V.; Mahesh, K. C.; Narasimhulu, M.; Venkateswarlu, Y. Simple and selective removal of the t-butyloxycarbonyl (Boc) protecting group on indoles, pyrroles, indazoles, and carbolines. *Synth. Commun.* **2007**, *37*, 281–287.

(11) Huang, J. R.; Qin, L.; Zhu, Y. Q.; Song, Q.; Dong, L. Multi-site cyclization via initial C-H activation using a rhodium(III) catalyst: rapid assembly of frameworks containing indoles and indolines. *Chem. Commun.* **2015**, *51*, 2844–2847.

(12) CCDC 2053243 contains the supplementary crystallographic data for this paper. These data are provided free of charge by the Cambridge Crystallographic Data Centre.

(13) (a) Allen, F. H.; Kennard, O.; Watson, D. G.; Brammer, L.; Orpen, A. G.; Taylor, R. Tables of bond lengths determined by X-ray and neutron diffraction. part 1. bond lengths in organic compounds. *J. Chem. Soc., Perkin Trans. 2* **1987**, *2*, S1. (b) Abbey, E. R.; Zakharov, L. N.; Liu, S.-Y. Crystal clear structural evidence for electron delocalization in 1,2-dihydro-1,2-azaborines. *J. Am. Chem. Soc.* **2008**, *130*, 7250–7252.

(14) (a) Zhang, C.; Zhang, L.; Sun, C.; Sun, W.; Liu, X. BN-phenanthrenes: synthesis, reactivity, and optical properties. *Org. Lett.* **2019**, *21*, 3476–3480. (b) Zhang, Q.; Sun, Z.; Zhang, L.; Li, M.; Zi, L.; Liu, Z.; Zhen, B.; Sun, W.; Liu, X. synthesis, structures, and properties of BN-dinaphthothiophenes: influence of B and N placement on photophysical properties and aromaticity. *J. Org. Chem.* **2020**, *85*, 7877–7883. (c) Zhang, J.; Liu, F.; Sun, Z.; Li, C.; Zhang, Q.; Zhang, C.; Liu, Z.; Liu, X. Synthesis, characterization and properties of aryl-fused bis-BN dihydropyrenes. *Chem. Commun.* **2018**, *54*, 8178–8181. (d) Li, C.; Liu, Y.; Sun, Z.; Zhang, J.; Liu, M.; Zhang, C.; Zhang, Q.; Wang, H.; Liu, X. Synthesis, characterization, and properties of bis-BN ullazines. *Org. Lett.* **2018**, *20*, 2806–2810.

(15) (a) Schleyer, P. v. R.; Maerker, C.; Dransfeld, A.; Jiao, H.; van Eikema Hommes, N. J. R. Nucleus-independent chemical shifts: a simple and efficient aromaticity probe. *J. Am. Chem. Soc.* **1996**, *118*, 6317–6318. (b) Chen, Z.; Wannere, C. S.; Corminboeuf, C.; Puchta, R.; Schleyer, P. v. R. Nucleus-independent chemical shifts (NICS) as an aromaticity criterion. *Chem. Rev.* **2005**, *105*, 3842–3888.

(16) Wang, X.; Zhuang, F.; Wang, X.; Cao, X.; Wang, J.; Pei, J. Synthesis, structure and properties of C3-symmetric heterosuperbenzene with three BN units. *Chem. Commun.* **2015**, *51*, 4368–4371.

(17) The energy level of ferrocene is assumed to be –4.80 eV versus vacuum Liu, Y.; Liu, M. S.; Jen, K.-Y. Synthesis and characterization of a novel and highly efficient light-emitting polymer. *Acta Polym.* **1999**, *50*, 105–108.

(18) Zhang, P. F.; Zhuang, F. D.; Sun, Z.; Lu, Y.; Wang, J. Y.; Pei, J. Rapid construction of fold-line-shaped BN-embedded polycyclic aromatic compounds through Diels–Alder reaction. *J. Org. Chem.* **2020**, *85*, 241–247.

(19) (a) Jäkle, F. Lewis acidic organoboron polymers. *Coord. Chem. Rev.* **2006**, *250*, 1107–1121. (b) Wade, C. R.; Broomsgrove, A. E. J.; Aldridge, S.; Gabbai, F. P. Fluoride ion complexation and sensing using organoboron compounds. *Chem. Rev.* **2010**, *110*, 3958–3984.

(20) (a) Jafarpour, F.; Rahiminejadan, S.; Hazrati, H. Triethanolamine-mediated palladium-catalyzed regioselective C-2 direct arylation of free NH-pyrroles. *J. Org. Chem.* **2010**, *75*, 3109–3112. (b) Nakazono, M.; Saita, K.; Oshikawa, Y.; Tani, K.; Nanbu, S.; Zaitso, K. Fluorescence properties of 2-aryl substituted indoles. *Spectrochim. Acta, Part A* **2011**, *78*, 905–908.

(21) Ballmann, G.; Rösch, B.; Harder, S. Stabilization of heteroleptic heavier alkaline earth metal complexes with an encapsulating dipyrromethene ligand. *Eur. J. Inorg. Chem.* **2019**, *2019*, 3683–3689.

(22) Yu, S. L.; Qi, L. J.; Hu, K.; Gong, J. L.; Cheng, T. X.; Wang, Q. Z.; Chen, J. X.; Wu, H. Y. The development of a palladium-catalyzed tandem addition/cyclization for the construction of indole skeletons. *J. Org. Chem.* **2017**, *82*, 3631–3638.